Lab on a Chip

Cite this: *Lab Chip*, 2012, **12**, 1710

www.rsc.org/loc

PAPER

Low-voltage electroosmotic pumps fabricated from track-etched polymer membranes†

Ceming Wang,[a] Lin Wang,[a] Xiaorui Zhu,[a] Yugang Wang[ab] and Jianming Xue*[ab]

Received 13th January 2012, Accepted 9th March 2012
DOI: 10.1039/c2lc40059f

Track-etched polymer membranes are used to realize low-voltage electroosmotic (EO) pumps. The nanopores in polycarbonate (PC) and polyethylene terephthalate (PET) membranes were fabricated by the track-etching technique, the pore diameter was controlled in the range of 100 to 250 nm by adjusting the etching time. The results show that these EO pumps can provide high flow rates at low applied voltages (2–5 V). The maximum normalized flow rate is as high as 0.12 ml min^{-1} V^{-1} cm^{-2}, which is comparable to the best values of previously demonstrated EO pumps. We attribute this high performance to the unique properties of the track-etched nanopores in the membranes.

1 Introduction

Microfluidics has broad application prospects in many fields, such as microelectromechanical systems, liquid drug delivery systems and micro-machines. A self-contained micropump, the package size of which is comparable to the volume of fluid to be pumped, is one of the most important components in these systems.[1]

So far, various micropumps have been fabricated and tested for microfluidics applications, and they have been extensively reviewed.[1–6] Among these micropumps, electroosmotic (EO) pumps operating on the principle of electroosmosis have received increasing attention in recent years.[5] An EO pump possesses several outstanding features: it can generate constant and pulse-free flows in a compact structure; the pumping flow magnitude and direction are convenient to control; it has no moving parts. EO pumps have been suggested to be used in many applications including high performance liquid chromatography,[7–9] micro flow injection analysis,[10,11] water management in fuel cells,[12,13] microelectronic equipment cooling,[14] drug delivery.[15]

High flow rate and low operation voltage are the key performance requirements for EO pumps to achieve compact design and efficient operation. However, traditional EO pumps require a very high driving voltage in the kilovolt range[5] to generate a sufficient flow rate, which in turn leads to several inherent problems of continuously operated EO pumps such as electrolytic gases, Joule heating, and eventually prohibits them from widespread applications due to the requirement of a high-voltage supply accessory.

In the past years, efforts to construct EO pumps with a high flow rate at a low applied voltage were reported.[16–21] The utilization of porous membranes for EO pumping is quite useful because they have a high porosity, a low channel tortuosity, and a short channel length (thickness). Because the channels are relatively short, high electric field strength is achieved when a low voltage is applied. Porous membranes such as porous silicon membrane,[16] porous anodic alumina membrane,[17,18] have been utilized to construct EO pumps. The refinement of electrodes such as coating electrodes on the porous membranes can reduce the distance between the two driving electrodes and provide a roughly uniform electric field. Recently, Ai *et al.*[19] built an EO pump with a platinum coated 60 μm thick porous anodic alumina membrane operating at 1–5 V with a maximum flow rate of 0.074 ml min^{-1} V^{-1} cm^{-2}. Shin *et al.*[20] constructed a nongassing pump by using consumed Ag/Ag_2O electrodes which operated well below 1.23 V, the thermodynamic threshold for electrolysis of water at 25 °C. In addition, a higher surface charge density can dramatically increase the zeta potential of channel walls,[22] which results in a higher pumping flow rate. Miao *et al.*[21] demonstrated that the flow rate of EO pumps based on silica coated porous anodic alumina membranes could reach 86 ml min^{-1} cm^{-2} under an operating voltage of 70 V. Nevertheless, the porous membranes mentioned above are difficult to be fabricated with a thinner thickness and these methods such as surface modification bring complexities in the fabrication of EO pumps.

Track-etched membranes fabricated by the track-etching technique[23,24] are widely used for process filtration, cell culture, and laboratory filtration.[25] The pore size can be tunable by changing the etching process, and the pore density can be varied from 10^{10} cm^{-2} down to a few pores cm^{-2}, which is determined by the number of incoming ions produced with accelerators or reactors. Polymers such as polyethylene terephthalate (PET) and

[a]*State Key Laboratory of Nuclear Physics and Technology, Peking University, Beijing 100871, People's Republic of China. E-mail: jmxue@pku.edu.cn; Fax: +86-10-62751875; Tel: +86-10-62758494*
[b]*Center for Applied Physics and Technology, Peking University, Beijing 100871, People's Republic of China*
† Electronic supplementary information (ESI) available. See DOI: 10.1039/c2lc40059f

polycarbonate (PC) are suitable for practical applications, due to their good mechanical strength[25] and high surface charge density.[26] A track-etched membrane can be easily fabricated with a thin polymer foil (~10 μm). Very recently, Jin *et al.*[27] studied EO flow through track-etched mica membranes containing asymmetric pores but did not put forth the possibility of using track-etched membranes for low-voltage EO pumping. We have performed a preliminary study on low-voltage EO pumping using track-etched PET membranes with double-conical pores,[28] which indicates that it is feasible to construct EO pumps using track-etched membranes.

In this work, we show that by using track-etched polymer membranes as pumping media, low-voltage EO pumps with high flow rate performance can be built. Two types of track-etched polymer membranes: PC and PET track-etched membranes with cylindrical nanopores and high porosity were fabricated by track-etching method. The potential applications of such EO pumps and some design issues for optimization of pump performance are also discussed. This research aims to demonstrate that the track-etched polymer membrane EO pumps can achieve high flow rate under a low applied voltage, while in a simple and compact structure.

2 Theory

EO pumping in porous membranes is modeled by treating the membrane as a parallel array of cylindrical pores of uniform pore radius a, with tortuosity τ, and porosity ψ. Flow rate dependence on applied voltage V_{app}, and pressure P, can then be described as,[29]

$$Q = \frac{\psi}{\tau}\left[-\frac{PAa^2}{8\mu L} - \frac{\varepsilon\zeta A V_{eff} f}{\mu L}\right] \quad (1)$$

where f is an integral of the form

$$f = \int_0^a \left(1 - \frac{\phi}{\zeta}\right)\frac{2r}{a^2}\mathrm{d}r \quad (2)$$

here V_{eff} is the effective applied axial voltage; ϕ is the electric potential; ζ, A, L are the zeta potential, the cross-sectional area, and the thickness of the membrane, respectively. f is the correction factor of the finite electrical double layer (EDL) effect on the flow rate; ε is the fluid permittivity; μ is the fluid viscosity. The model can be applied to our track-etched polymer membranes with $\tau = 1$. Because the diameters of the nanopores used in our experiments are larger than 100 nm, therefore the continuum theory is still valid.

The maximum flow rate Q_{max} generated across the porous membrane is obtained from eqn (1) for the condition of zero counter pressure. The maximum pressure P_{max} is obtained for the condition of zero net flow rate ($Q = 0$). The maximum flow rate and pressure are as follows:

$$Q_{max} = -\psi A\varepsilon\zeta V_{eff} f/(\mu L) \quad (3)$$

$$P_{max} = -8\varepsilon\zeta V_{eff} f/a^2 \quad (4)$$

Another important characteristic of the EO pump is thermodynamic efficiency, which is defined as

$$\eta = \frac{PQ}{V_{app}I} = \frac{1}{4}\frac{P_{max}Q_{max}}{V_{app}I} \quad (5)$$

The efficiency is the ratio of the useful pressure work, PQ, to the applied electrical work, $V_{app}I$. The useful pressure work, PQ, is determined experimentally from flow rate *versus* pressure and PQ is equal to $1/2P_{max} \times 1/2Q_{max}$. These equations allow the prediction of the performance for an EO pump, given pore radius, zeta potential, macroscopic dimensions of the pumping media, and working fluid chemistry.

The solution to the integral f can be obtained by solving the Poisson–Boltzmann equation for electrical potential. Using the Debye–Hückel approximation, the correction factor, f, can be expressed as,

$$f = 1 - \frac{2I_1(a/\lambda)}{a/\lambda I_0(a/\lambda)} \quad (6)$$

Debye–Hückel approximation is only valid for low to moderate zeta potentials. Here, I_0 and I_1 are the zeroth and first order modified Bessel function of the first kind, respectively. λ is Debye length that can be given by,

$$\lambda = \sqrt{\frac{\varepsilon k_B T}{2e^2 z n}} \quad (7)$$

where n, k_B, T, e, and z are the counterion concentration of bulk solution, the Boltzmann number, the temperature of the liquid, the electron charge, and the valence number of the counterion, respectively. The ionic concentration of the deionized (DI) water used in the present study is approximately $n = 1.0 \times 10^{-5}$ M, which leads to a Debye length of 100 nm.

Eqn (3) highlights the advantage of utilization of thin porous membranes for EO pumps, which shows that the thin thickness of the porous membrane lowers V_{app} for a given Q. The track-etched polymer membranes are much thinner ($L = 12$ μm for PET and $L = 10$ μm for PC) than other porous membranes used in previous works,[16–19,21] hence, higher electric field strength can be achieved when the same voltage is applied.

3 Materials and fabrication

In this section, we describe the fabrication and characterization of track-etched PC and PET membranes.

3.1 Fabrication

The nanopores in the membranes were prepared by the track-etching technique[23,24] as shown in Fig. 1, which is based on the irradiation of a material with swift heavy ions and subsequent chemical etching. The pore size can be controlled by the etching time, and the number of ions per unit area determines the number of damage tracks and, hence, pores.

In this study, we worked with 10 μm thick PC foils and 12 μm thick PET foils. These polymer films were irradiated by ^{238}U with an energy of 11.4 MeV per nucleon at the linear accelerator UNILAC at the Gesellschaft für Schwerionenforschung (GSI) Darmstadt, Germany. The number of the incoming ions per unit area is 5×10^8 ions cm^{-2} for PC foils and 10^8 ions cm^{-2} for PET foils. Before etching, UV irradiation was performed on each side of the PC (for 0.5 h) and PET (for 1 h) samples to increase the

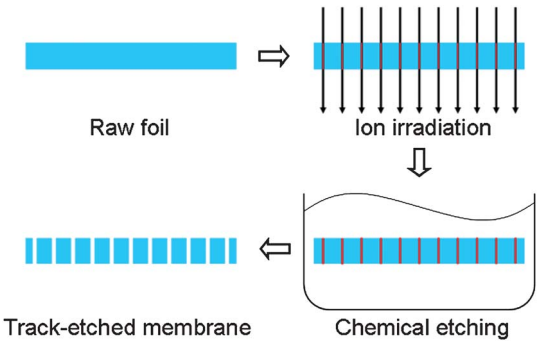

Fig. 1 Schematic of the fabrication process of track-etched membrane by the track-etching technique.

sensitivity of the further chemical etching. PC foils were etched from both sides simultaneously with 6 M NaOH aqueous solution at a temperature of 50 °C. Under these conditions, the pore diameter scales linearly with etching time at a rate of ~10 nm min^{-1}. We etched the PC foils for 10, 15 and 20 min so that the diameters of the cylindrically shaped nanopores are approximately 100, 150 and 200 nm, respectively. Nanopores in the PET foils were prepared by etching from both sides in 2 M NaOH at a temperature of 60 °C and the diameters of these nanopores are about 250 nm.

3.2 Characterization

For any application or theoretical description of track-etched membranes, it is important to know their characteristic parameters including pore density, pore shape and pore diameter. The pore density is determined by the number of incoming ions per unit area, which is 5×10^8 ions cm^{-2} for PC foils and 10^8 ions cm^{-2} for PET foils in this study. We checked the pore densities with SEM through the counting process. The resulting relative statistical errors are typically less than 20%.

In our experiments, conductometric measurements on single pores showed that their pore diameters scaled with etching time, which yield an average etching rate of 10 nm min^{-1} for PC samples under the described etching condition (see ESI†). This etching rate was used as a reference for etching track-etched PC membranes with specific pore diameters. The actual pore diameters were then confirmed with SEM observations. The pore diameters of 100, 150 and 200 nm reported for the track-etched PC membranes were all checked with SEM (Fig. S2, ESI†). The same method was also used to fabricate the track-etched PET membranes with a pore diameter of around 250 nm. Those samples with undesired pore diameters were discarded in our experiments. Fig. 2a shows the track-etched PC membrane with a pore diameter of 100 nm.

Under the described etching conditions, the resulting track-etched PC and PET membranes consist of an array of straight, cylindrical pores with a tortuosity approaching unity. We prepared cleavages of our samples to reveal their shapes. SEM observations show that the resulting nanopores in track-etched PC and PET membranes are cylindrical and parallel to each other, as illustrated in Fig. 2b. The method for preparing cleavages is presented in the ESI.†

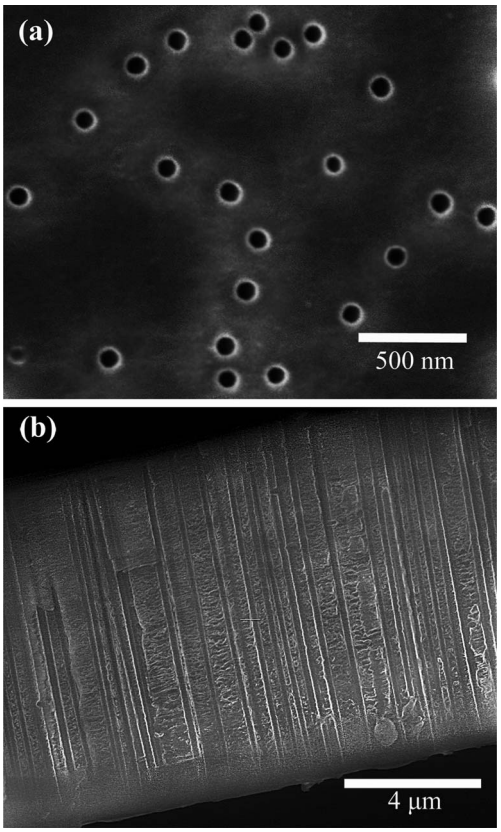

Fig. 2 (a) SEM micrograph of a track-etched PC membrane with pore density of 5×10^8 cm^{-2}. The pore diameter is around 100 nm; (b) Cross-sectional SEM image of a cleavage for track-etched PC membrane with 5×10^8 pores cm^{-2} and pore diameter of approximately 150 nm. The SEM image shows that the nanopores are cylindrical and parallel to each other and the thickness of the membrane is 10 μm.

The porosity, ψ, can be estimated by pore density, v, and diameter, d, as

$$\psi = \frac{1}{4} v \pi d^2 \tag{8}$$

In the present study, twenty samples in total were investigated experimentally, and these samples were divided into four groups according to their pore diameters. Three groups of track-etched PC membranes with pore density of 5×10^8 cm^{-2} have average pore diameters of 100, 150, and 200 nm, respectively. The other group of track-etched PET membranes has an average pore diameter of 250 nm and a pore density of 10^8 cm^{-2}.

4 Experimental details

The pump assembly is depicted in the schematic shown in Fig. 3. The pump consists of two chambers separated by the track-etched polymer membrane. The pump housing was fabricated from plexiglass. The Au mesh electrodes with 0.02 mm diameter wires and center-to-center spacing of 0.05 mm were made by coating a 400 nm thick layer of Au on the stainless mesh. The Au mesh electrodes have direct contact with the thin membranes to reduce the electric voltage drop in the reservoir and to provide a roughly uniform electric field. Another advantage of using

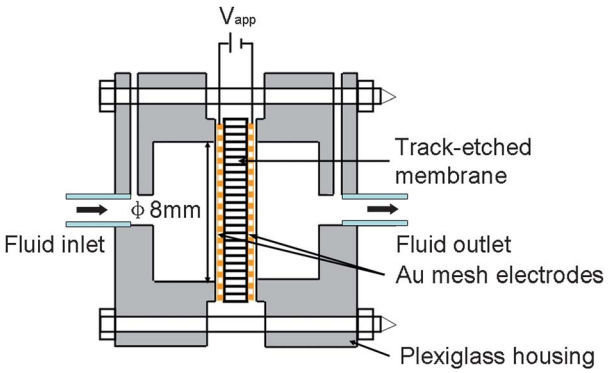

Fig. 3 Schematic of the EO pump fabricated from track-etched membrane. The pump has a 130 μm thick and 0.5 cm^2 active cross-sectional area.

mesh electrodes is that the mesh electrodes can serve as supporting frames to withstand the pressure produced by the EO effect. The track-etched polymer membrane as well as the Au mesh electrodes were sandwiched between two halves of the plexiglass housing. The diameter of the effective pumping area of the membrane is 8 mm.

For all experiments, DI water was used as the working fluid in order to reduce the ion current of the pump during operation and increase thermodynamic efficiency. The fluid within the nanopore was driven by the electric field provided by a picoammeter (Model 6487, Keithley Instruments Inc., Cleveland, OH). In this study, the experimental setup for pump performance characterization has a similar configuration to that used by Yao *et al.*[16] The pumping flow rates were measured using a balance with 1 mg precision upstream of the pump. The fluid inlet and outlet were connected with two liquid reservoirs. The back pressure was varied by changing the hydraulic head of a downstream liquid reservoir so we can apply favorable pressure differences across the pump. The magnitude of the back pressure was estimated by the fluid height difference between the downstream and upstream reservoirs.

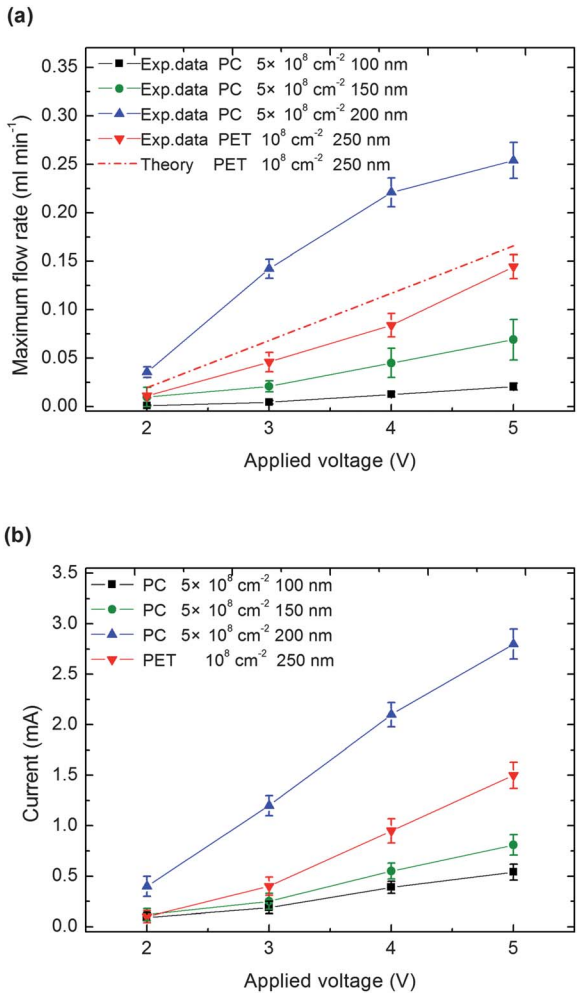

Fig. 4 The measured maximum flow rate (a), current (b) *versus* applied voltage for EO pumps fabricated from three track-etched PC membranes with pore density of 5×10^8 cm^{-2} and different pore diameters (100, 150 and 200 nm) as well as a track-etched PET membrane with pore density of 10^8 cm^{-2} and pore diameter of 250 nm. Shown together with the data is the model prediction for the track-etched PET membrane (dashed line).

5 Results and discussion

In this section, we present measurements of pump performance in the form of flow rate, current and pressure, and the results are compared with the analytical model predictions. In addition, some design issues for optimization of pump performance and the potential applications of track-etched polymer membrane EO pumps are also discussed.

5.1 Flow rate and current

Four groups of as-prepared track-etched polymer membranes were tested in our pump systems. The maximum flow rate, Q_m, and current, I, were measured at applied voltages ranging from 2 to 5 V. To keep our figures simple, we only show the data of a typical sample for each group, while other samples present similar behavior. Fig. 4a shows the dependence of the maximum pump flow rate on the applied voltage. The theoretical calculations with the parameters of the PET sample are also shown for comparison. A maximum flow rate of 0.254 ± 0.019 ml min^{-1} is achieved when a voltage of 5 V is applied. For all the samples, the maximum flow rate shows a linear increasing trend with increasing applied voltage. Fig. 4b shows the corresponding current for the measurements shown in Fig. 4a. The current also shows linear dependence on the applied voltage.

We find that for the track-etched PC membranes with identical pore density (5×10^8 cm^{-2}), samples with larger pore diameters yield higher flow rates (see Fig. 4a). This is mainly due to two factors. Obviously, a larger pore diameter would mean a larger porosity for a given membrane. Furthermore, the integral f in eqn (3) increases as the electrokinetic radius (a/λ) increases especially for $a/\lambda \leq 10$ which means a larger driving force for flow.[29] The pore diameters of the three membranes ranging from 100 to 200 nm are comparable to the Debye length (100 nm) of DI water for our studies so that the corresponding electrokinetic radius (a/λ) is less than 10.

Because the flow rate depends linearly on the applied voltage as well as the pumping area, a better figure of merit for the pumping performance is the normalized flow rate, which is in the

unit of millilitre per minute per voltage per unit area. Fig. 5 shows the comparison of our result in terms of normalized flow rate with the reported values in the past decades.[11,14,16,17,19,20,30–37] The maximum value in our study is 0.12 ml min^{-1} V^{-1} cm^{-2}, it was obtained with the track-etched PC membrane of pore diameter 200 nm. Our result is higher than the normalized flow rates of most other EO pumps shown in Fig. 5, while it was achieved under a low operating voltage of 4 V. There is only one comparable study[19,20] which used a few tenths of a volt to reach the same order of normalized flow rate. Our previous study[28] evaluated the pumping performance simply in terms of flow rate and current. But other parameters, such as pressure and thermodynamic efficiency, are also important considerations. This study has characterized the pumping performance in more detail. Power consumption is critical for practical applications. With the data shown in Fig. 4a and 4b, the flow rate per power consumption ($Q_m/(IV_{app})$) can be calculated, which varies between 7 to 30 ml min^{-1} W^{-1} (a typical value for EO pumps[16]) for the small and large pore pumps, respectively.

The low operating voltage is due to the thin thickness of the track-etched polymer membranes, which are around 10 μm in thickness. By applying a low operating voltage (4 V), it could provide a high electric field (0.33 MV m^{-1}) to drive the EO flow. Many previous studies had employed a much higher voltage to provide a comparable electric field (*e.g.* 0.33 MV m^{-1} at 20 V,[17] 0.1 MV m^{-1} at 6 kV[35]). Moreover, the high zeta potential of the track-etched nanopore, due to its high surface charge,[26] enhances the EO flow through these nanopores. The high pore density, low tortuosity, and uniform pore diameter accompanying the track-etched membrane is also one of the benefits of the present low-voltage EO pump with high flow rate performance. Consequently, it is possible to achieve an appreciable flow rate under a low operating voltage by using track-etched polymer membranes.

Fig. 4a also shows the linear dependence of the maximum flow rate with applied voltage for the track-etched PET membrane with a pore diameter of 250 nm. Shown together with the data are model predictions for the maximum flow rate. The measured flow rate is several times higher than the result achieved in our previous study,[28] which used track-etched PET membrane containing double-conical pores with lower porosity. This result indicates that straightforward pore shape and higher porosity are beneficial for performance optimization. Eqn (3) was used to calculate the maximum flow rate while assuming a zeta potential of PET[38] of −36.2 mV. As discussed by Yao *et al.*,[30] the applied voltage, V_{app}, would get distributed as the decomposition potential associated with the electrode reactions and the resistances associated with electrode-to-pump spacing. We estimated the decomposition potential from a preliminary calibration experiment. The value can be determined from the extrapolation of the current *versus* voltage response of the pump to the zero current point. The average decomposition potential measured in our experiments was 1.6 V. The value was used to calculate effective voltage, V_{eff}.

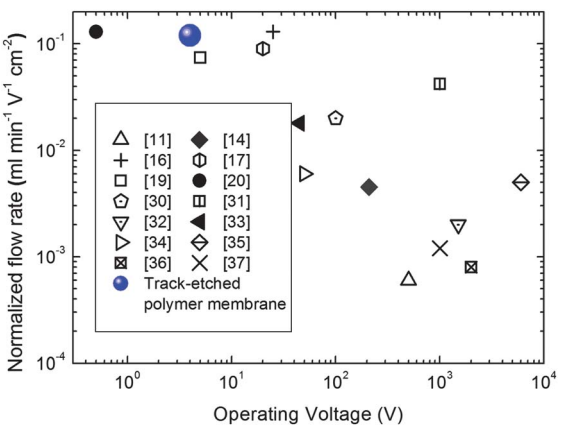

Fig. 5 Comparison of the normalized flow rate obtained from track-etched polymer membrane EO pump against flow rates reported in the literature.

Comparing the experimental data with the model prediction, we can find that the theoretical results slightly overestimate the flow rate by ~18%. One possible reason is that, in our calculation, the coefficient f in eqn (6) is modeled based on the Debye–Hückel approximation which is strictly valid for low to moderate zeta potentials below 25 mV.[39] Despite the discrepancy, the analytical model can capture the major trend and is useful in estimating the flow rate performance. The analytical model is also more straightforward and effective than the numerical model used in our previous study,[28] especially for cylindrical pores.

We use measurements of Q_m to estimate the zeta potential, ζ, of track-etched PC membranes (see eqn (3)). A curve fit of the experimental data points of three PC samples gives $\zeta = -23 \pm 5$ mV, which shows reasonable agreement with the results by Lettmann *et al.*[40] We can use this value to estimate the flow rate performance of track-etched PC membranes with different pore densities and diameters, as discussed in the last section.

To examine the pump-to-pump repeatability, four groups of membranes varying the polymer material, the pore density and the pore diameter were investigated to ensure the data reproducibility. EO pumps fabricated from each group of membranes showed similar pumping capability. The relative deviation of the measurement is typically less than 20% in terms of flow rate.

These pumps showed stable pumping performance in short-term operation (less than 30 min). The reason that these pumps cannot provide long-term stable pumping performance is that the pH drops during continuous operation, which decreases the surface charge and thus the EO flow. A long-term operation can be achieved by improving the pump configuration. The approach for long-term operation of EO pumps has been studied by Brask *et al.*[41]

5.2 Pressure performance

The results presented above have been for a zero pressure load. However, many applications have a finite pressure load. We measured the flow rate against fixed back pressure loads between 0 to 0.7 kPa using the as-prepared track-etched PC membrane with a pore diameter of 200 nm. Fig. 6 shows data for the flow rate under different pressure loads at an applied voltage of 5 V. The maximum pressure, P_{max}, achieved by this membrane is 0.7 kPa. Then the thermodynamic efficiency of the corresponding EO pump estimated by eqn (5) is 0.005%. We believe that the other two track-etched PC membranes with smaller pore

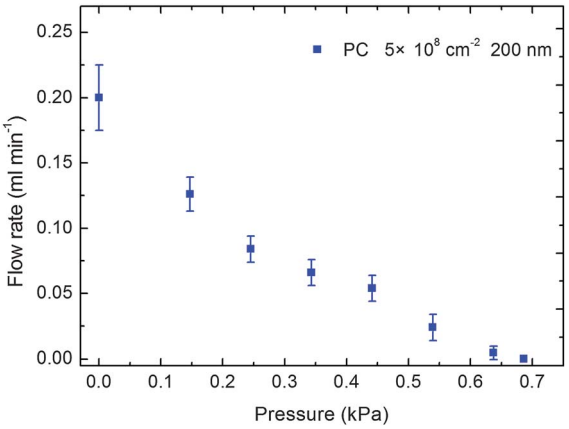

Fig. 6 Flow rate *versus* back pressure for the EO pump fabricated from track-etched PC membrane with a pore density of 5×10^8 cm^{-2} and pore diameter of approximately 200 nm at an applied voltage of 5 V.

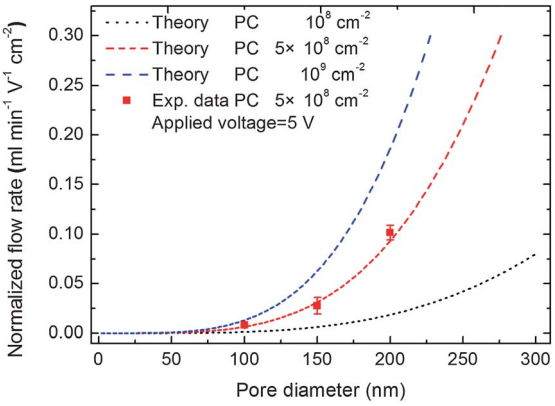

Fig. 7 Theoretically predicted normalized flow rates of the track-etched PC membrane EO pump as a function of the pore diameter with three different pore densities: 10^8, 5×10^8 and 10^9 cm^{-2} at an applied voltage of 5 V. Shown together with the data are the experimental results.

diameters can provide a larger pressure capacity. The reason for this is that pressure varies as the inverse of the square of the pore diameter as indicated by eqn (4). A check on the pumping pressure indicates that the predicted maximum pressure using eqn (4) can be several times higher than the experimental result. A likely reason for the discrepancy in pressure prediction is that the model uses a single average pore diameter, while the actual membrane has a distribution of pore diameters.

5.3 Performance optimization and potential applications

Track-etched membranes offer distinct advantages over conventional membranes due to their precisely determined structure. Their pore size and density can be varied in a controllable manner so that these feature parameters can be optimized to maximize both flow rate and pressure capacity. Higher pore density can be coupled with decreasing pore diameter to achieve higher pressure capacity for a given flow rate. Alternatively, increasing pore density for a given pore diameter results in higher porosity and flow rate while maintaining a constant pressure capacity; but this leads to pore overlapping and poor mechanical strength of the membrane. We suggest that the pore size and pore density be chosen as a tradeoff between flow rate and pressure capacity. Fig. 7 shows the prediction of normalized flow rates of the track-etched PC membrane EO pump as a function of pore diameter with three pore densities at an applied voltage of 5 V. Shown together with the data are the experimental results. The flow rate linearly increases with the increasing porosity. Compared with our previous study,[28] track-etched polymer membranes with straightforward pore shape and higher porosity can provide higher flow rates. We believe that the normalized flow rate of the present EO pump can be further improved by using a membrane with even larger porosity, as well as working fluids with appropriate ion concentrations.

High surface charge density and thin thickness make using virgin track-etched membrane to achieve a high flow rate at a low applied voltage feasible. Compared with previous studies, the common approaches, such as surface modification to enhance flow rate, can be eliminated, which in turn simplifies the fabrication process of the present EO pump. We think these features will facilitate their integration into micro- or nanofluidics chips which is necessary for these chips to reach widespread applications because using micro- or nanofluidics chips is often not straightforward. The instrumentation around these chips often consists of bulky equipment (*e.g.*, high-voltage power supplies, syringe pumps). Moreover, the present low-voltage EO pumps are also capable of providing a pressure capacity for applications such as drug delivery. For example, the drugs can be subcutaneously infused at modest, typically $\leq$1 kPa, pressure.[20] The low-cost fabrication of this type of pump is beneficial for their application in a daily replaced drug delivery system containing the infused drug such as insulin solution. In addition, the track-etched polymer membrane EO pumps are also promising for applications which have high demands with respect to flow rate such as microelectronics cooling.

6 Conclusion

We have successfully shown that the utilization of track-etched polymer membranes enables EO pumping to achieve flow rates that are higher than most of those reported in the literature at a low voltage. In addition to a low operating voltage, the simple and cost-effective fabrication of track-etched polymer membrane EO pumps also makes them attractive for future applications in micro- or nanofluidics chips. These EO pumps are also capable of providing pressure/flow rate capacity sufficient for applications such as drug delivery and microelectronics cooling.

We believe that the flow rate may be further improved by using membranes with even larger pore diameters, pore densities and different pore shape. One outstanding feature of track-etched nanopores is that the pore geometry can be tunable. Pores with conical and double-conical shapes have been successfully fabricated in the track-etched membrane. Earlier research[21,27] has pointed out that the geometry of the pores has an important effect on the pumping performance. More systematic studies based on the track-etched membrane EO pump can help us to understand and optimize this effect. We believe that utilizing this feature may endue track-etched polymer membrane EO pumps with some new functions.

Acknowledgements

This work is financially supported by the National Natural Science Foundation of China (Grant No. 10975009) and by the Ministry of Science and Technology of China (Grant No. 2010CB832904). The material group of GSI, Germany is gratefully acknowledged for providing the irradiated foils.

Notes and references

1 D. J. Laser and J. G. Santiago, *J. Micromech. Microeng.*, 2004, **14**, R35–R64.
2 C. Zhang, D. Xing and Y. Li, *Biotechnol. Adv.*, 2007, **25**, 483–514.
3 B. Iverson and S. Garimella, *Microfluid. Nanofluid.*, 2008, **5**, 145–174.
4 A. Nisar, N. Afzulpurkar, B. Mahaisavariya and A. Tuantranont, *Sens. Actuators, B*, 2008, **130**, 917–942.
5 X. Wang, C. Cheng, S. Wang and S. Liu, *Microfluid. Nanofluid.*, 2009, **6**, 145–162.
6 S. Qian and H. H. Bau, *Mech. Res. Commun.*, 2009, **36**, 10–21.
7 V. Pretorius, B. J. Hopkins and J. D. Schieke, *J. Chromatogr., A*, 1974, **99**, 23–30.
8 L. Chen, J. Ma and Y. Guan, *Microchem. J.*, 2003, **75**, 15–21.
9 L. Chen, J. Ma and Y. Guan, *J. Chromatogr., A*, 2004, **1028**, 219–226.
10 S. Liu and P. K. Dasgupta, *Anal. Chim. Acta*, 1992, **268**, 1–6.
11 W. Gan, L. Yang, Y. He, R. Zeng, M. L. Cervera and M. Guardia, *Talanta*, 2000, **51**, 667–675.
12 C. R. Buie, J. D. Posner, T. Fabian, S. W. Cha, D. Kim, F. B. Prinz, J. K. Eaton and J. G. Santiago, *J. Power Sources*, 2006, **161**, 191–202.
13 C. R. Buie, D. Kim, S. Litster and J. G. Santiago, *Electrochem. Solid-State Lett.*, 2007, **10**, B196–B200.
14 L. Jiang, J. Mikkelsen, J. M. Koo, D. Huber, S. Yao, L. Zhang, P. Zhou, J. G. Maveety, R. Prasher, J. G. Santiago, T. W. Kenny and K. E. Goodson, *IEEE Trans. Compon. Packag. Technol.*, 2002, **25**, 347–355.
15 L. Chen, J. Choo and B. Yan, *Expert Opin. Drug Delivery*, 2007, **4**, 119–129.
16 S. H. Yao, A. M. Myers, J. D. Posner, K. A. Rose and J. G. Santiago, *J. Microelectromech. Syst.*, 2006, **15**, 717–728.
17 Y. F. Chen, M. C. Li, Y. H. Hu, W. J. Chang and C. C. Wang, *Microfluid. Nanofluid.*, 2008, **5**, 235–244.
18 S. K. Vajandar, D. Xu, D. A. Markov, J. P. Wikswo, W. Hofmeister and D. Li, *Nanotechnology*, 2007, **18**, 1–9.
19 Y. Ai, S. E. Yalcin, D. Gu, O. Baysal, H. Baumgart, S. Qian and A. Beskok, *J. Colloid Interface Sci.*, 2010, **350**, 465–470.
20 W. Shin, J. M. Lee, R. K. Nagarale, S. J. Shin and A. Heller, *J. Am. Chem. Soc.*, 2011, **133**, 2374–2377.
21 J. Y. Miao, Z. L. Xu, X. Y. Zhang, N. Wang, Z. Y. Yang and P. Sheng, *Adv. Mater.*, 2007, **19**, 4234–4237.
22 V. V. Berezkin, V. I. Volkov, O. A. Kiseleva, N. V. Mitrofanova and V. D. Sobolev, *Adv. Colloid Interface Sci.*, 2003, **104**, 325–331.
23 R. L. Fleischer, P. B. Price and R. M. Walker, *Nuclear Tracks in Solids. Principles and Applications*, University of California Press, Berkeley, 1975.
24 B. E. Fischer and R. Spohr, *Rev. Mod. Phys.*, 1983, **55**, 907–948.
25 P. Apel, *Radiat. Meas.*, 2001, **34**, 559–566.
26 J. M. Xue, Y. B. Xie, Y. Yan, K. Jin and Y. G. Wang, *Biomicrofluidics*, 2009, **3**, 022408–022408.
27 P. Jin, H. Mukaibo, L. P. Horne, G. W. Bishop and C. R. Martin, *J. Am. Chem. Soc.*, 2010, **132**, 2118–2119.
28 C. Wang, L. Wang and J. M. Xue, *Nucl. Instrum. Methods Phys. Res., Sect. B*, 2012, DOI: 10.1016/j.nimb.2011.12.032.
29 S. H. Yao and J. G. Santiago, *J. Colloid Interface Sci.*, 2003, **268**, 133–142.
30 S. H. Yao, D. E. Hertzog, S. Zeng, J. C. Mikkelsen Jr and J. G. Santiago, *J. Colloid Interface Sci.*, 2003, **268**, 143–153.
31 C. H. Chen and J. G. Santiago, *J. Microelectromech. Syst.*, 2002, **11**, 672–683.
32 O. T. Guenat, D. Ghiglione, W. E. Morf and N. F. de Rooij, *Sens. Actuators, B*, 2001, **72**, 273–282.
33 T. E. McKnight, C. T. Culbertson, S. C. Jacobson and J. M. Ramsey, *Anal. Chem.*, 2001, **73**, 4045–4049.
34 J. A. Tripp, F. Svec, J. M. J. Frechet, S. Zeng, J. C. Mikkelsen Jr. and J. G. Santiago, *Sens. Actuators, B*, 2004, **99**, 66–73.
35 P. Wang, Z. Chen and H. C. Chang, *Sens. Actuators, B*, 2006, **113**, 500–509.
36 S. Zeng, C. H. Chen, J. C. Mikkelsen Jr. and J. G. Santiago, *Sens. Actuators, B*, 2001, **79**, 107–114.
37 S. Zeng, C. H. Chen, J. G. Santiago, J. R. Chen, R. N. Zare, J. A. Tripp, F. Svec and J. M. J. Frechet, *Sens. Actuators, B*, 2002, **82**, 209–212.
38 P. Deéjardin, E. N. Vasina, V. V. Berezkin, V. D. Sobolev and V. I. Volkov, *Langmuir*, 2005, **21**, 4680–4685.
39 C. L. Rice and R. Whitehead, *J. Phys. Chem.*, 1965, **69**, 4017–4024.
40 C. Lettmann, D. Möckel and E. Staude, *J. Membr. Sci.*, 1999, **159**, 243–251.
41 A. Brask, J. P. Kutter and H. Bruus, *Lab Chip*, 2005, **5**, 730–738.